

## Article

# Feasibility Studies for the Measurement of Open-Charm Mesons at ALICE-3 Using Decay Channels with Neutral Mesons and Photons in the Final State

Mikhail Malaev<sup>1,2</sup> and Victor Riabov<sup>1,2,\*</sup> 

<sup>1</sup> Petersburg Nuclear Physics Institute Named by B.P.Konstantinov of NRC “Kurchatov Institute”, Gatchina 188300, Russia

<sup>2</sup> Moscow Institute of Physics and Technology, Dolgoprudny 141701, Russia

\* Correspondence: riabov\_vg@pnpi.nrcki.ru; Tel.: +7-813-714-6131

**Abstract:** ALICE-3 is being designed as a next-generation heavy-ion experiment to be operated at the high-luminosity Large Hadron Collider. With luminosities higher by a factor of fifty, ALICE-3 will be able to study properties of quark–gluon matter with probes and precision which were previously unavailable due to small cross sections, high background levels, and insufficient detector sensitivity. In particular, the properties of hot and dense QCD matter will be studied by measuring production cross sections, flow coefficients, azimuthal angular correlations and nuclear modification factors for open-charm hadrons. In this contribution, we present the results of feasibility studies for the measurement of ground and excited states of open-charm mesons in decay channels  $D^0 \rightarrow K^- + \pi^+ + \pi^0$ ,  $D^*(2007)^0 \rightarrow D^0 + \gamma$  and  $D^*(2010)^\pm \rightarrow D^0 + \pi^\pm$  in pp, p-Pb and Pb-Pb collisions at LHC energies using the ALICE-3 experimental setup. We formulate the main requirements for the selection of particles and their combinations to ensure reliable signal extraction in a wide transverse momentum range and estimate the minimum size of the required data samples. The results obtained are also compared to previous findings for the open-charm measurements in different decay channels.



**Citation:** Malaev, M.; Riabov, V. Feasibility Studies for the Measurement of Open-Charm Mesons at ALICE-3 Using Decay Channels with Neutral Mesons and Photons in the Final State. *Particles* **2023**, *6*, 364–372. <https://doi.org/10.3390/particles6010018>

Academic Editors: Peter Senger, Arkadiy Taranenko and Ilya Selyuzhenkov

Received: 30 December 2022

Revised: 8 February 2023

Accepted: 10 February 2023

Published: 17 February 2023



**Copyright:** © 2023 by the authors. Licensee MDPI, Basel, Switzerland. This article is an open access article distributed under the terms and conditions of the Creative Commons Attribution (CC BY) license (<https://creativecommons.org/licenses/by/4.0/>).

**Keywords:** relativistic heavy-ion collisions; open charm; heavy flavor; particle reconstruction

## 1. Introduction

The goal of the heavy-ion program at the LHC is to determine the properties of strongly interacting matter in the regime of extremely high temperatures and near-zero net-baryon densities. To pursue this physics program beyond the reach of modern experiments, the novel ALICE-3 detector with high read-out rate, superb pointing resolution and excellent tracking and particle identification over a large acceptance and using advanced silicon detectors was proposed to be operated at the high-luminosity Large Hadron Collider at CERN after 2030 [1]. The main part of the detector is a silicon pixel tracker, with sensors arranged in barrel layers and forward disks, installed in the volume of 80 cm radius and  $\pm 4$  m length around the interaction point. The outer tracker consists of eight cylindrical layers, with each of the layers contributing about 1% of the material’s radiation length. The relative momentum resolution with the magnetic field of  $B = 2$  T provided by the superconducting magnet system is  $\sim 0.6\%$  at mid-rapidity. To optimize the pointing resolution, the first three tracking layers are placed inside the LHC beam pipe and have radial distances of 0.5 cm, 1.2 cm and 2.5 cm from the interaction point. For particle identification, time-of-flight (TOF) and ring-imaging Cherenkov (RICH) detectors cover a broad momentum range, both relying on novel silicon timing and photon sensors. With a time resolution of 20 ps, a TOF layer outside of the tracker at a radius of 85 cm allows the identification of electrons and hadrons up to transverse momenta of 0.5 GeV/c and 2 GeV/c for p/K separation, respectively. For particles below 0.3 GeV/c, which do not

reach this TOF layer, an inner TOF layer is foreseen at a radius of 20 cm. An aerogel-based RICH detector with a refractive index of  $n = 1.03$  and an angular resolution of 1.5 mrad is located behind the TOF and enables the separation of electrons and pions up to 2 GeV/ $c$  and of protons from  $e$ ,  $p$  and  $K$  up to 14 GeV/ $c$ . Photon detection and lepton identification at higher momentum are provided by an electromagnetic calorimeter, which is located behind the RICH and covers the whole barrel acceptance and exploits established detector technologies.

Collisions of heavy nuclei at the LHC provide unique experimental access to the hottest and longest-lived quark–gluon plasma available in the laboratory, with abundant production of heavy flavor probes. The aim of the measurement of the ground and excited states of open-charm mesons in ultrarelativistic heavy-ion collisions at the LHC is to study the production mechanisms of heavy  $c$ -quarks (particle yields), the involvement of heavy flavor particles in the collective system expansion (particle flow coefficients) as well as the scattering and energy loss of  $c$ -quarks traversing the dense and hot partonic medium produced in the collisions (azimuthal angular correlations, nuclear modification factors) [2–10]. The ALICE-3 experiment is specifically optimized for the measurement of open heavy-flavor hadrons and heavy-flavor correlations in heavy-ion collisions over a wide rapidity interval down to zero transverse momentum. Results of feasibility studies for the measurement of  $D^0$  mesons in  $D^0 \rightarrow \pi^+K^-$  channel in the momentum range  $p_T < 16$  GeV/ $c$  are presented in [1]. In the study, the  $D^0$  candidates were selected using secondary vertex topological criteria and particle identification selections based on the TOF and RICH signals to suppress combinatorial background. It is demonstrated that ALICE-3 will reconstruct  $D^0$  mesons with unprecedented accuracy in a wide rapidity range ( $|\eta| < 4$ ) with signal-to-background (S/B) ratio reaching 10–80 in the momentum range 1–16 GeV/ $c$  at mid-rapidity. ALICE-3 demonstrates much better efficiency for the reconstruction of low- $p_T$   $D^0$  mesons compared with the modern ALICE-2 detector. The achieved S/B ratio exceeds that in ALICE-2 by a factor of  $\sim 200$  at 2 GeV/ $c$ , and by a factor of  $\sim 2$  at 16 GeV/ $c$ . The performance of the ALICE-3 detector for the reconstruction of high- $p_T$   $D^0$  mesons is not discussed in [1]. Qualitatively, the large acceptance of the ALICE-3 detector will remain an important advantage, but the importance of the pointing resolution and hadron identification will diminish in this momentum range.

In this contribution, we present the results of feasibility studies for the measurement of  $D^0$ ,  $D^*(2007)^0$  and  $D^*(2010)^\pm$  mesons in pp, p-Pb and Pb-Pb collisions at top LHC energies using the ALICE-3 experimental setup, with a focus on the measurement of high- $p_T$  mesons. The following and the charge conjugate decays of open-charm mesons have been considered:  $D^0 \rightarrow K^- + \pi^+ + \pi^0$  with BR =  $(14.4 \pm 0.5)\%$ , taking into account decays through intermediate resonances,  $D^*(2007)^0 \rightarrow D^0 + \gamma$  with BR =  $(64.7 \pm 0.9)\%$  and  $D^*(2010)^\pm \rightarrow D^0 + \pi^\pm$  with BR =  $(67.7 \pm 0.5)\%$  [11]. Hereafter, we refer to  $D^0$ ,  $D^*(2007)^0$  and  $D^*(2010)^\pm$  mesons as D mesons for brevity. All these decay channels have a neutral  $\pi^0$  meson in the final state, which can be reconstructed in the  $\pi^0 \rightarrow \gamma + \gamma$  decay channel using the electromagnetic calorimeter of the ALICE-3 experiment. The decay channels are characterized by relatively large branching ratios, and parent particles can be reconstructed using data samples collected with a trigger condition of having at least one high-energy signal in the calorimeter (presumably from a high-energy photon). Such a trigger can significantly enhance the effective integrated luminosity compared with minimum bias data samples traditionally used for the measurement of D mesons in the decay channels with two or more charged particles in the final state. In this study, the realistic event generator is used to simulate the signals and background particles. Both signal and background are traced through the ALICE-3 experimental setup using a simplified approach, which includes geometrical and detector efficiency filtering of the particles, smearing of particle momenta, energies and coordinates based on the estimated performance of the detector subsystems. The simplified approach is used in the absence of the Geant-based framework for the full ALICE-3 detector simulation to produce first-look estimations, which would need finer clarifications in the future. The measurement of open-charm mesons in the decay channels

with neutral pions in the final state would be an extension of  $\omega(782) \rightarrow \pi^+ + \pi^- + \pi^0$  analyses previously performed in pp, p-A and A-A collisions at RHIC and the LHC in the energy range  $\sqrt{s_{NN}} = 0.2\text{--}7$  TeV [12–14].

## 2. Feasibility Studies

The yields of  $D^0$  and  $D^*(2010)^\pm$  mesons were measured in the ALICE experiment in pp, p-Pb and Pb-Pb collisions at LHC energies [2–5]. These measurements are characterized by rather large uncertainties and wide transverse momentum ( $p_T$ ) and centrality intervals. In this work, the Pythia 8 (v. 8.14, Monash 2013 tune for pp collisions, with “Angatyr” option for p-Pb and Pb-Pb collisions) [15–18] event generator was used to estimate production yields of D mesons and background particles in pp, p-Pb and Pb-Pb collisions at LHC energies. To validate the event generator, D-meson yields predicted by the event generator were compared with the yields measured by the ALICE experiment. In Figure 1, one can see examples of such a comparison for the case of pp collisions at  $\sqrt{s} = 13$  TeV and different centrality Pb-Pb collisions at  $\sqrt{s_{NN}} = 5.02$  TeV. In pp and p-Pb collisions (not shown), the event generator underestimates the production of D mesons by up to 50%. This precision is sufficient for the estimation of the capability of ALICE-3 to reconstruct D mesons, making such estimations rather conservative. For Pb-Pb collisions, the event generator adequately reproduces the measured D-meson spectra in peripheral (60–80%) and semicentral (30–50%) collisions at  $p_T > 2\text{--}3$  GeV/c, but overestimates the yields in most central collisions (0–20%), where numbers in brackets are for centrality binning in percentage of a total inelastic nucleus–nucleus cross section. For the estimations, the predicted D-meson spectra simulated in central Pb-Pb collisions were downscaled to bring them in accordance with the measured ones. At this  $p_T$ -differential,  $D^*(2010)^\pm/D^0$  ratios measured and simulated in pp, p-Pb and Pb-Pb collisions were found to be in good agreement. It is interesting to note that the measured and predicted  $p_T$ -differential  $D^0/\pi^0$  ratios increased with  $p_T$  and reached  $D^0/\pi^0 \sim 1$  at  $p_T > 6\text{--}7$  GeV/c for all collision systems (corresponding to  $D^*(2007)^0/\pi^0$  and  $D^*(2010)^\pm/\pi^0$  ratios of  $\sim 0.5$ ). This indicates rather high production rates of D mesons at high transverse momentum, which should facilitate the measurements. For example, the  $\omega(782)/\pi^0$  ratio was measured equal to  $\sim 0.8$  in the same momentum range.

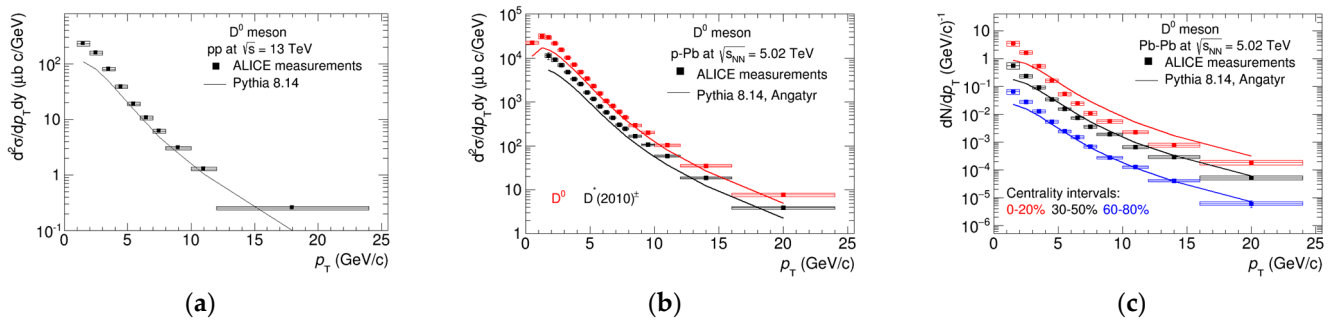


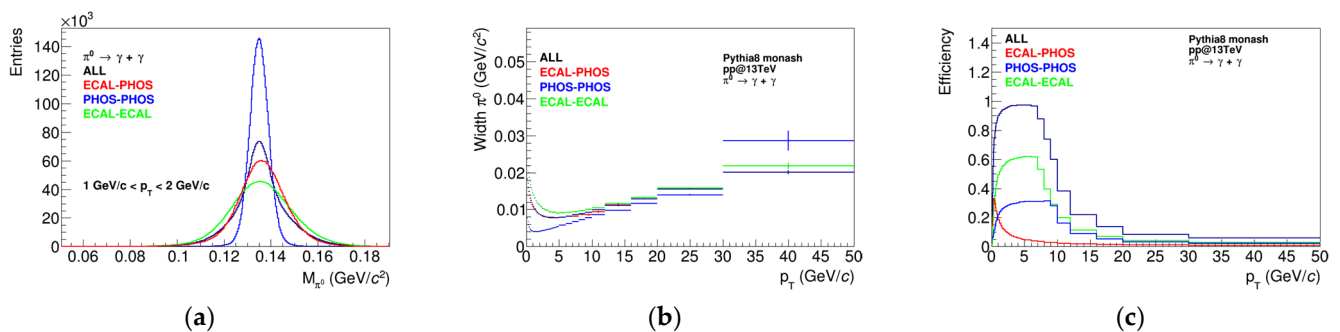
**Figure 1.**  $D^0$  transverse momentum spectra measured by ALICE experiment in pp collisions at  $\sqrt{s} = 13$  TeV [4] (a), p-Pb (b) and 0–20%, 30–50% and 60–80% central Pb-Pb collisions at  $\sqrt{s_{NN}} = 5.02$  TeV [2] (c). Statistical and systematic uncertainties of the measurements are shown with error bars and boxes, respectively. Measurements are compared to predictions of the Pythia 8 event generator shown with solid lines, which connect predicted particle yields in the same  $p_T$  intervals as in the data.

In the following studies, we estimate ALICE-3 capabilities for the reconstruction of D-meson yields using the same collision energies and  $p_T$  intervals as in the published ALICE papers. The obtained results will remain valid for the collision energies expected for the operation of ALICE-3 ( $\sqrt{s} = 14$  TeV for pp,  $\sqrt{s_{NN}} = 8.8$  TeV for p-Pb and  $\sqrt{s_{NN}} = 5.52$  TeV for Pb-Pb), given the degree of the used simplifications. At the same time, this approach

preserves the possibility of direct comparison with the published results. At this stage, the studies were limited to the midrapidity region,  $|\eta| < 1$ .

The ALICE-3 experimental setup is described well in [1]. For reconstruction and identification of the charged particles, it was required that they cross all eight layers of the central tracking system and fall within the acceptance of the TOF and RICH detectors. The subsystem acceptance, efficiency of charged particle track reconstruction and momentum resolution as a function of particle momentum and rapidity were applied as reported in [1] for a magnetic field of  $B = 2$  T. Tracks from decays of D mesons were counted as identified assuming  $3\text{-}\sigma$  particle identification selections in the TOF and RICH detectors. For background particles, the  $3\text{-}\sigma$  probabilities for the separation of charged  $e/\pi$ ,  $\pi/K$  and  $K/p$  pairs in the TOF and RICH subsystems as a function of particle momentum and rapidity were used as defined in [1]. The impurities from hadron misidentification beyond  $3\text{-}\sigma$  selections were also considered; for example, a small fraction of background pions were erroneously identified as kaons even for the charged pion tracks, which laid within the  $3\text{-}\sigma$  range of  $\pi/K$  separation. For reconstruction of  $\pi^0$  mesons it was required that both daughter photons fell within the acceptance of the electromagnetic calorimeter, which is built using two different technologies. The central part of the calorimeter ( $|\eta| < 0.33$ ) consists of  $\text{PbWO}_4$  crystals with a segmentation of  $2.2 \times 2.2 \text{ cm}^2$  and energy resolution of  $\delta E/E = 1\% + 2\%/\sqrt{E(\text{GeV})}$ . The forward parts of the calorimeter ( $0.22 < |\eta| < 1.5$ ) are built of PbSc sampling towers with a segmentation of  $3 \times 3 \text{ cm}^2$  and energy resolution of  $\delta E/E = 1\% + 10\%/\sqrt{E(\text{GeV})}$ . Hereafter we refer to central and forward parts of the calorimeter as PHOS and ECAL for simplicity.

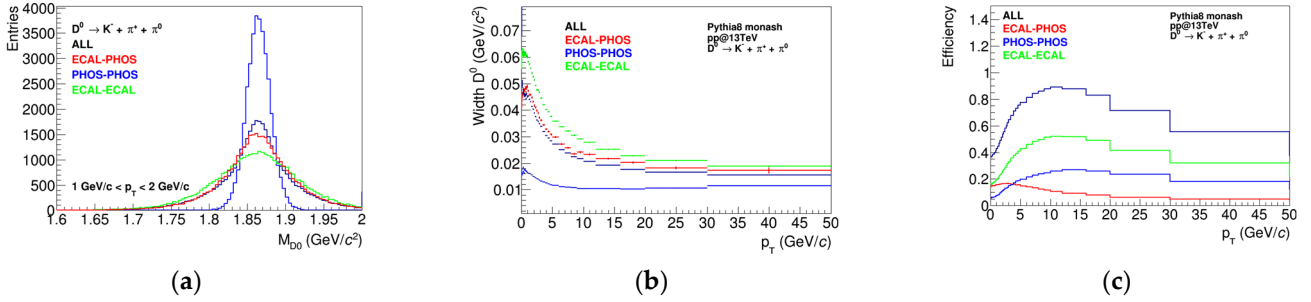
Figure 2 shows ALICE-3 performance for the reconstruction of neutral pions as a function of particle transverse momentum. The internal radius of the calorimeter is only 1.15 m, which has the following consequences: (1) the width of the reconstructed  $\pi^0$  peaks in the invariant mass distributions is defined by energy resolution at low momenta and by spatial resolution at high momenta, and the width of  $\pi^0$  peaks increases at  $p_T > 3\text{--}5 \text{ GeV}/c$ ; (2) reconstruction efficiency for  $\pi^0$  decreases at  $p_T > 6\text{--}8 \text{ GeV}/c$  due to increasing probability of shower merging for two daughter photons. Two showers could be separated if the minimum distance between their centers exceeded  $1.5 \times 2.2$  (3) cm for the PHOS (ECAL). Only  $\pi^0$  decays with both daughter photons reconstructed in the electromagnetic calorimeter were accepted in the analysis. At  $p_T < 10 \text{ GeV}/c$ , the reconstructed  $\pi^0$  width shows a strong dependence on the particular detector technology, with the smallest width observed for the PHOS due to much better energy resolution and minor importance of the spatial resolution at low energies due to large  $\gamma\text{--}\gamma$  opening angles. At higher momenta, the reconstructed  $\pi^0$  width becomes comparable for the PHOS and ECAL due to different interplay between the energy and spatial resolution.



**Figure 2.** Invariant mass spectra for the reconstructed  $\pi^0 \rightarrow \gamma + \gamma$  decays (a), the width of reconstructed  $\pi^0$  peaks (b) and reconstruction efficiency for  $\pi^0$  (c) as a function of transverse momentum for the cases of measuring photons in the PHOS and ECAL parts of the electromagnetic calorimeter.

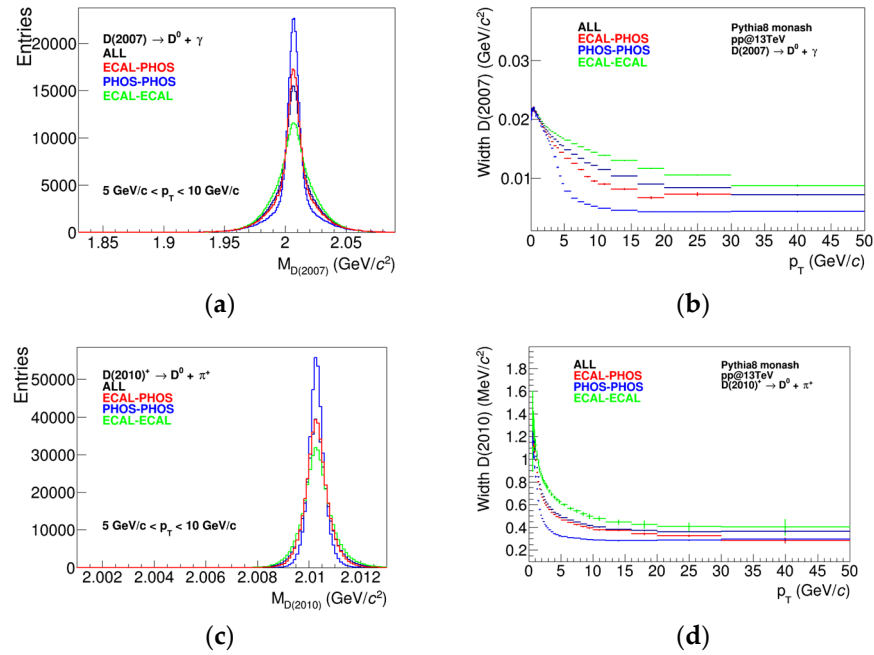
Figure 3 shows the detector performance for the reconstruction of  $D^0$  mesons in the  $D^0 \rightarrow K^- + \pi^+ + \pi^0$  decay channel. The widths of  $D^0$  peaks in the invariant mass distributions are defined by the accuracy of reconstruction of daughter  $\pi^0$  mesons and have

different values for the cases of measuring photons in the PHOS and ECAL parts of the electromagnetic calorimeter. The width of  $D^0$  mesons decreases with increasing transverse momentum and flattens out at the level of 10–20  $\text{MeV}/c^2$  at high  $p_T$ . The reconstruction efficiency for  $D^0$  meson increases with  $p_T$ , reaches a maximum at  $p_T \sim 10 \text{ GeV}/c$  and then slowly decreases due to increasing probability of shower merging for photons from  $\pi^0$  decays. The effect of cluster merging is not as pronounced for  $D^0$  mesons because the same transverse momentum of a parent particle can be provided with a wide range of  $\pi^0$  momenta.



**Figure 3.** Invariant mass spectra for the reconstructed  $D^0 \rightarrow K^- + \pi^+ + \pi^0$  decays (a), the width of reconstructed  $D^0$  peaks (b) and reconstruction efficiency for  $D^0$  (c) as a function of transverse momentum for the cases of measuring photons in the PHOS and ECAL parts of the electromagnetic calorimeter.

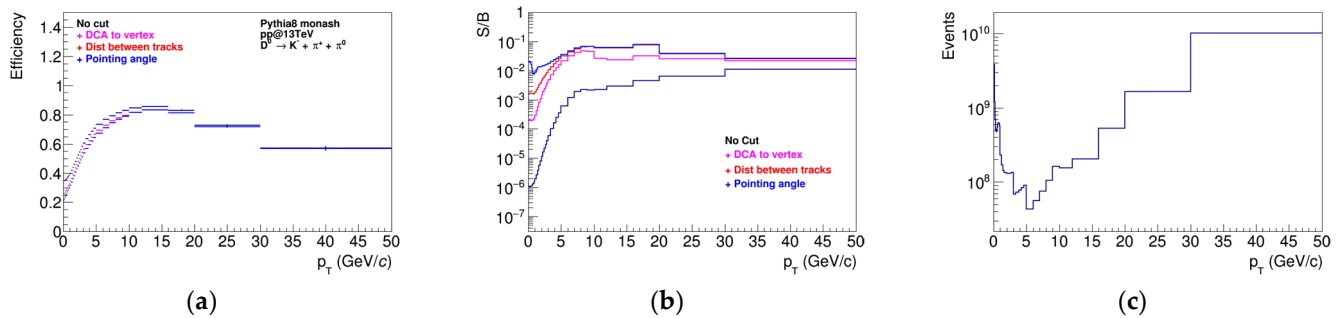
Figure 4 shows examples of the invariant mass spectra reconstructed for decays of excited states  $D^*(2007)^0 \rightarrow D^0 + \gamma$  and  $D^*(2010)^\pm \rightarrow D^0 + \pi^\pm$  as well as dependences of the widths of the reconstructed meson peaks on particle momentum. Due to the small difference in the total masses of the daughter and parent particles, the reconstructed meson peaks are very narrow, with a width of 1–10  $\text{MeV}/c^2$ , which should result in better signal-to-background ratios and easier peak extraction in the invariant mass distributions.



**Figure 4.** Invariant mass distributions from  $D^*(2007)^0 \rightarrow D^0 + \gamma$  (a) and  $D^*(2010)^\pm \rightarrow D^0 + \pi^\pm$  (c) decays and width of the reconstructed  $D^*(2007)^0$  (b) and  $D^*(2010)^\pm$  (d) peaks as a function of transverse momentum for the cases of measuring photons in the PHOS and ECAL parts of the electromagnetic calorimeter.

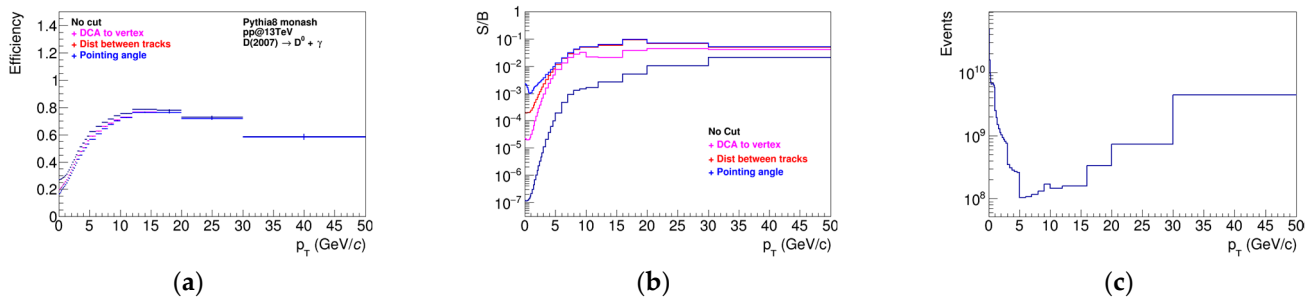
The presented results suggest high efficiency of the ALICE-3 experimental setup for the reconstruction of signals from decays of D mesons. The next step would be the evaluation of detector capabilities for the rejection of combinatorial background and estimation of the needed statistics for the measurement of D mesons. To suppress the combinatorial background in events with high multiplicity, several criteria for the selection of single particles and their combinations were developed: (1) Since  $D^0$  mesons decay away from the primary vertex, reconstructed tracks of charged daughter pions and kaons should not point to the vertex. The characteristic resolution,  $\sigma(p_T)$ , of the ALICE-3 experimental setup for determining the distance between the reconstructed charged particle track and the primary vertex is presented in [1], and ranges from twenty to a few microns, depending on the transverse momentum of the particle. When selecting the charged particle tracks, it was required that their distance to the primary vertex exceeded  $2 \cdot \sigma(p_T)$ . (2) At  $D^0$  meson decay vertex, the distance between the daughter charged particle tracks must be equal to zero within the measurement uncertainties. When selecting pairs of charged tracks, it was required that the minimum distance between them did not exceed  $50 \mu\text{m}$ . (3) The momentum vector of the triplet  $K^- \pi^+ \pi^0$  from decay of the  $D^0$  meson must point from the reconstructed secondary decay vertex to the primary interaction vertex. It was required that the cosine of the angle between the reconstructed  $D^0$ -meson momentum vector and a straight line connecting the primary and secondary vertices was larger than 0.99.

Figure 5 shows how the selections described above affect the  $D^0$ -meson reconstruction efficiency and the S/B ratio as a function of the particle transverse momentum. The distributions are presented for pp collisions at  $\sqrt{s} = 13 \text{ TeV}$ . The  $D^0$ -meson reconstruction efficiency moderately decreases at low transverse momentum while the S/B ratio increases significantly and reaches a value greater than or equal to  $\sim 10^{-2}$ . Figure 5 also shows the estimated number of events required to measure  $D^0$ -meson yields with a statistical uncertainty of 10%. To measure the production spectrum in the momentum range up to  $50 \text{ GeV}/c$ , it is sufficient to collect about ten billion events. ALICE-3 plans to collect a data set with equivalent statistics of  $\sim 3 \text{ fb}^{-1}$  per year, which corresponds to  $\sim 200$  billion pp collisions. Such a number of events will be sufficient to measure the  $D^0$  production spectrum with a statistical uncertainty of  $\sim 2\%$  in the specified  $p_T$  bins.



**Figure 5.** Reconstruction efficiency (a) and signal-to-background ratio (b) for  $D^0$  mesons with different track selections. Number of events required to measure  $D^0$ -meson production with a statistical uncertainty of 10% in the whole momentum range (c). Examples are shown for the case of pp collisions at  $\sqrt{s} = 13 \text{ TeV}$ .

Similar estimations for the case of  $D^*(2007)^0 \rightarrow D^0 + \gamma$  and  $D^*(2010)^\pm \rightarrow D^0 + \pi^\pm$  decays are shown in Figures 6 and 7, respectively. Lower per-event yields of the excited states are partly compensated by much narrower widths of the reconstructed peaks in the invariant mass distributions, which overall results in S/B ratios comparable to those previously reported for  $D^0$  mesons. As a result, about the same statistics are required to measure  $D^0$ ,  $D^*(2007)^0$  and  $D^*(2010)^\pm$  mesons with comparable uncertainties in the momentum range  $p_T > 1 \text{ GeV}/c$ .



**Figure 6.** Reconstruction efficiency (a) and signal-to-background ratio (b) for  $D^*(2007)^0$  mesons with different track selections. Number of events required to measure  $D^*(2007)^0$ -meson production with a statistical uncertainty of 10% in the whole momentum range (c). Examples are shown for the case of pp collisions at  $\sqrt{s} = 13$  TeV.

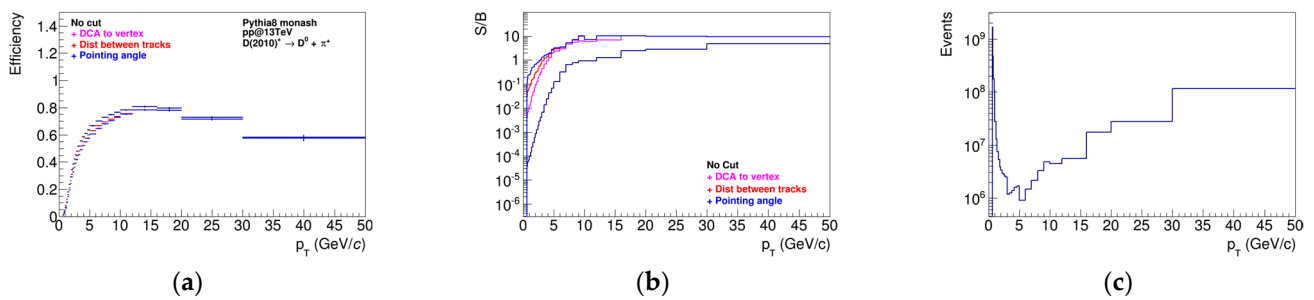


**Figure 7.** Reconstruction efficiency (a) and signal-to-background ratio (b) for  $D^*(2010)^\pm$  mesons with different track selections. Number of events required to measure  $D^*(2010)^\pm$ -meson production with statistical uncertainty of 10% in the whole momentum range (c). Examples are shown for the case of pp collisions at  $\sqrt{s} = 13$  TeV.

Estimations for S/B ratios and the number of events needed to measure  $D^0$ ,  $D^*(2007)^0$  and  $D^*(2010)^\pm$  mesons in p-Pb and Pb-Pb collisions at  $\sqrt{s_{NN}} = 5.02$  TeV were also obtained using the following assumptions. In the simplified simulation approach, the effect of high occupancy in high-multiplicity events is not accounted for. As a result, the reconstruction efficiencies evaluated for pp collisions at  $\sqrt{s} = 13$  TeV and presented in Figures 5–7 remain valid for heavier collision systems. The S/B ratios for different collision systems were estimated by scaling the ratios shown in Figures 5–7 by  $R_{AA} \cdot N_{coll} / N_{part}^2$ , where  $R_{AA}$  is a pT-dependent factor of nuclear modification, while  $N_{part}$  and  $N_{coll}$  are the numbers of participants and binary nucleon–nucleon collisions [2,3,5]. The expression is based on the assumption that heavy flavor is produced in hard scattering processes that scale with  $N_{coll}$ , while the mean event multiplicity scales with  $N_{part}$ . This results in S/B ratios better than  $2 \cdot 10^{-3}$  and  $10^{-4}$  in p-Pb and 0–20% central Pb-Pb collisions. With known per-event yields of D mesons one can estimate a required number of events to measure the production of D mesons in the pT range up to 50 GeV/c with a statistical uncertainty of ~10%: 12 billion p-Pb events and 2 (3) (7) billion Pb-Pb collisions in the centrality intervals 0–20% (30–50%) (60–80%), respectively. ALICE-3 plans to collect integrated luminosities of  $5.6 \text{ nb}^{-1}$  per month and  $33.6 \text{ nb}^{-1}$  in two years for Pb-Pb collisions, which are equivalent to 45 and 260 billion Pb-Pb collisions, respectively, that can reduce the statistical uncertainty of measurements to ~3%.

### 3. Conclusions

Estimates are obtained for the yields of D mesons and background particles in pp, p-Pb and Pb-Pb collisions at LHC energies using the Pythia 8 event generator. The generator predictions for pp, p-Pb and peripheral Pb-Pb collisions are in good agreement with the measurements of the ALICE experiment. For central Pb-Pb collisions, Pythia 8 over predicts

D-meson yields; predictions of the event generator can be used after the application of appropriate weights.

Methods for the identification of D mesons and the suppression of combinatorial background for  $D^0 \rightarrow K^- + \pi^+ + \pi^0$ ,  $D^*(2007)^0 \rightarrow D^0 + \gamma$  and  $D^*(2010)^\pm \rightarrow D^0 + \pi^\pm$  decays are developed and provide S/B ratios better than  $10^{-2}$ ,  $2 \cdot 10^{-3}$  and  $10^{-4}$  in pp, p-Pb and 0–20% central Pb-Pb collisions at LHC energies. The reported S/B ratios are significantly smaller than those reported for the measurement in the  $D^0 \rightarrow \pi^+ K^-$  decay channel in the overlap region,  $p_T < 16$  GeV/c [1]. This can be explained by a higher level of combinatorial background in decays with more particles in the final state, by a wider width of the reconstructed peaks in the invariant mass distributions and lower efficiency of topological cuts in the decays where the trajectory of the neutral daughter particle cannot be precisely estimated. Direct comparison with the  $D^0 \rightarrow \pi^+ K^-$  channel at higher momenta is not possible due to lack of data for comparison. The performance of ALICE-3 for the measurement of  $D^0 \rightarrow K^- + \pi^+ + \pi^0$ ,  $D^*(2007)^0 \rightarrow D^0 + \gamma$  and  $D^*(2010)^\pm \rightarrow D^0 + \pi^\pm$  can be further improved by accepting  $\pi^0$  mesons, which are measured as single merged clusters in the calorimeter. This approach has been successfully used by the ALICE experiment in the measurement of  $\pi^0$  mesons at high  $p_T$  up to 200 GeV/c [19]. This will significantly increase the reconstruction efficiency for  $\pi^0$  mesons and the parent D mesons at high momentum. Better background suppression can also be achieved with more advanced simulations, which would more realistically account for the track curvature in the magnetic field and the spatial resolution of the central tracker. Another argument in favor of the measurement of D mesons in decay channels with neutral particles would be a larger sampled luminosity with a dedicated event selection trigger. However, solid estimations for the gain in the sampled luminosity for different collision systems is not currently possible because of large uncertainties in the expected performance of the accelerator and detector data acquisition system.

Measurements in  $D^0 \rightarrow K^- + \pi^+ + \pi^0$ ,  $D^*(2007)^0 \rightarrow D^0 + \gamma$  and  $D^*(2010)^\pm \rightarrow D^0 + \pi^\pm$  decay channels will be possible with ALICE-3. The expected signal significances will be noticeably larger compared with the published ALICE results. However, it is not yet clear if the presented measurements will have any advantages over more traditional measurements in the decay channels with only charged particles in the final state carried out using minimum-bias data samples.

**Author Contributions:** Conceptualization, methodology, validation and writing, V.R.; software, data analysis and visualization, M.M. All authors have read and agreed to the published version of the manuscript.

**Funding:** This work was supported by the Russian Science Foundation grant 22-42-04405.

**Institutional Review Board Statement:** Not applicable.

**Informed Consent Statement:** Not applicable.

**Data Availability Statement:** Not applicable.

**Acknowledgments:** The presented results were obtained using the resources of the PIK Data Center of the NRC «Kurchatov Institute»—PNPI.

**Conflicts of Interest:** The authors declare no conflict of interest. The funders had no role in the design of the study; in the collection, analysis, or interpretation of data; in the writing of the manuscript; or in the decision to publish the results.

## References

1. Abelev, B.; Adam, J.; Adamová, D.; Aggarwal, M.M.; Agnello, M.; Agostinelli, A.; Agrawal, N.; Ahammed, Z.; Ahmad, N.; Masoodi, A.A.; et al. Letter of intent for ALICE 3: A next-generation heavy-ion experiment at the LHC. *arXiv* **2022**, arXiv:2211.02491.
2. Acharya, S.; Adamová, D.; Adler, A.; Adolfsson, J.; Rinella, G.A.; Agnello, M.; Agrawa, N.; Ahammed, Z.; Ahmad, S.; Ahn, S.U.; et al. Prompt  $D^0$ ,  $D^+$ , and  $D^{*+}$  production in Pb-Pb collisions at  $\sqrt{s_{NN}} = 5.02$  TeV. *JHEP* **2022**, *1*, 174.

3. Acharya, S.; Acosta, F.T.; Adamová, D.; Adolfsson, J.; Aggarwal, M.M.; Rinella, G.A.; Agnello, M.; Agrawa, N.; Ahammed, Z.; Ahn, S.U.; et al. Measurement of  $D^0$ ,  $D^+$ ,  $D^{*+}$  and  $D_s^+$  production in Pb-Pb collisions at  $\sqrt{s_{NN}} = 5.02$  TeV. *JHEP* **2018**, *1810*, 174.
4. Acharya, S.; Adamová, D.; Adler, A.; Adolfsson, J.; Rinella, G.A.; Agnello, M.; Agrawa, N.; Ahammed, Z.; Ahmad, S.; Ahn, S.U.; et al. Measurement of prompt  $D^0$ ,  $\Lambda_c^+$ , and  $\Sigma_c^{0,++}(2455)$  production in pp collisions at  $\sqrt{s} = 13$  TeV. *Phys. Rev. Lett.* **2022**, *128*, 012001. [[CrossRef](#)] [[PubMed](#)]
5. Acharya, S.; Adamová, D.; Adhya, S.P.; Adler, A.; Adolfsson, J.; Aggarwal, M.M.; Rinella, G.A.; Agnello, M.; Agrawal, N.; Ahammed, Z.; et al. Measurement of prompt  $D^0$ ,  $D^+$ ,  $D^{*+}$ , and  $D_s^+$  production in p-Pb collisions at  $\sqrt{s_{NN}} = 5.02$  TeV. *JHEP* **2019**, *12*, 92.
6. Acharya, S.; Adamová, D.; Adler, A.; Adolfsson, J.; Rinella, G.A.; Agnello, M.; Agrawa, N.; Ahammed, Z.; Ahmad, S.; Ahn, S.U.; et al. Investigating charm production and fragmentation via azimuthal correlations of prompt D mesons with charged particles in pp collisions at  $\sqrt{s_{NN}} = 13$  TeV. *Eur. Phys. J. C* **2022**, *82*, 335. [[CrossRef](#)]
7. Acharya, S.; Adamová, D.; Adler, A.; Adolfsson, J.; Rinella, G.A.; Agnello, M.; Agrawa, N.; Ahammed, Z.; Ahmad, S.; Ahn, S.U.; et al. Azimuthal correlations of prompt D mesons with charged particles in pp and p-Pb collisions at  $\sqrt{s_{NN}} = 5.02$  TeV. *Eur. Phys. J. C* **2020**, *80*, 979. [[CrossRef](#)]
8. Acharya, S.; Adamová, D.; Adler, A.; Adolfsson, J.; Aggarwal, M.M.; Rinella, G.A.; Agnello, M.; Agrawal, N.; Ahammed, Z.; Ahmad, S.; et al. Transverse-momentum and event-shape dependence of D-meson flow harmonics in Pb-Pb collisions at  $\sqrt{s_{NN}} = 5.02$  TeV. *Phys. Lett. B* **2021**, *813*, 136054. [[CrossRef](#)]
9. Acharya, S.; Acosta, F.T.; Adamová, D.; Adler, A.; Adolfsson, J.; Aggarwal, M.M.; Rinella, G.A.; Agnello, M.; Agrawal, N.; Ahammed, Z.; et al. Event-shape engineering for the D-meson elliptic flow in mid-central Pb-Pb collisions at  $\sqrt{s_{NN}} = 5.02$  TeV. *JHEP* **2019**, *2*, 150.
10. Adam, J.; Adamová, D.; Aggarwal, M.M.; Rinella, G.A.; Agnello, M.; Agrawal, N.; Ahammed, Z.; Ahn, S.U.; Aimo, I.; Aiola, S.; et al. Centrality dependence of high- $p_T$  D meson suppression in Pb-Pb collisions at  $\sqrt{s_{NN}} = 2.76$  TeV. *JHEP* **2015**, *11*, 205. [[CrossRef](#)]
11. Particle Data Group; Zyla, P.A.; Barnett, R.M.; Beringer, J.; Dahl, O.; Dwyer, D.A.; Groom, D.E.; Lin, C.-J.; Lugovsky, K.S.; Pianori, E.; et al. Review of Particle Physics. *Prog. Theor. Exp. Phys.* **2020**, *2020*, 083C01.
12. Acharya, S.; Adamová, D.; Adler, A.; Adolfsson, J.; Aggarwal, M.M.; Agha, S.; Rinella, G.A.; Agnello, M.; Agrawa, N.; Ahammed, Z.; et al. Production of  $\omega$  mesons in pp collisions at  $\sqrt{s} = 7$  TeV. *Eur. Phys. J. C* **2020**, *80*, 1130.
13. Adare, A.; Afanasiev, S.; Aidala, C.; Ajitanand, N.N.; Akiba, Y.; Al-Bataineh, H.; Al-Jamel, A.; Alexander, J.; Angerami, A.; Aoki, K.; et al. [PHENIX Collaboration] Production of  $\omega$  mesons in p+p, d+Au, Cu+Cu, and Au+Au collisions at  $\sqrt{s_{NN}} = 200$  GeV. *Phys. Rev. C* **2011**, *84*, 044902. [[CrossRef](#)]
14. Adler, S.S.; Afanasiev, S.; Aidala, C.; Ajitanand, N.N.; Akiba, Y.; Al-Jamel, A.; Alexander, J.; Aoki, K.; Aphenetche, L.; Armendariz, R.; et al. [PHENIX Collaboration] Production of omega mesons at Large Transverse Momenta in p + p and d + Au Collisions at  $\sqrt{s_{NN}} = 200$  GeV. *Phys. Rev. C* **2007**, *75*, 051902. [[CrossRef](#)]
15. Sjostrand, T.; Mrenna, S.; Skands, P.Z. A brief introduction to PYTHIA 8.1. *Comput. Phys. Commun.* **2008**, *178*, 852–867. [[CrossRef](#)]
16. Bierlich, C.; Chakraborty, S.; Desai, N.; Gellersen, L.; Helenius, I.; Ilten, P.; Lönnblad, L.; Mrenna, S.; Prestel, S.; Preuss, C.T.; et al. A comprehensive guide to the physics and usage of PYTHIA 8.3. *SciPost Phys. Codebases* **2022**, *8*. [[CrossRef](#)]
17. Skands, P.; Carrazza, S.; Rojo, J. Tuning PYTHIA 8.1: The Monash 2013 Tune. *Eur. Phys. J. C* **2014**, *74*, 3024. [[CrossRef](#)]
18. Bierlich, C.; Gustafson, G.; Lönnblad, L.; Shah, H. The Angantyr model for Heavy-Ion Collisions in PYTHIA8. *JHEP* **2018**, *10*, 134. [[CrossRef](#)]
19. Acharya, S.; Adamová, D.; Adler, A.; Adolfsson, J.; Rinella, G.A.; Agnello, M.; Agrawa, N.; Ahammed, Z.; Ahmad, S.; Ahn, S.U.; et al. Nuclear modification factor of light neutral-meson spectra up to high transverse momentum in p-Pb collisions at  $\sqrt{s_{NN}} = 8.16$  TeV. *Phys. Lett. B* **2022**, *827*, 136943. [[CrossRef](#)]

**Disclaimer/Publisher’s Note:** The statements, opinions and data contained in all publications are solely those of the individual author(s) and contributor(s) and not of MDPI and/or the editor(s). MDPI and/or the editor(s) disclaim responsibility for any injury to people or property resulting from any ideas, methods, instructions or products referred to in the content.